

# Automatic Segmentation of Skin Lesion Images Using Evolution Strategies

Xiaojing Yuan<sup>a,\*</sup>, George Zouridakis<sup>a,b,c</sup>, Ning Situ<sup>c</sup>,

<sup>a</sup>*University of Houston, Engineering Technology Department, Houston, TX 77204*

<sup>b</sup>*University of Houston, Texas Learning Computation Center, Houston, TX 77204*

<sup>c</sup>*University of Houston, Computer Science Department, Houston, TX 77204*

---

## Abstract

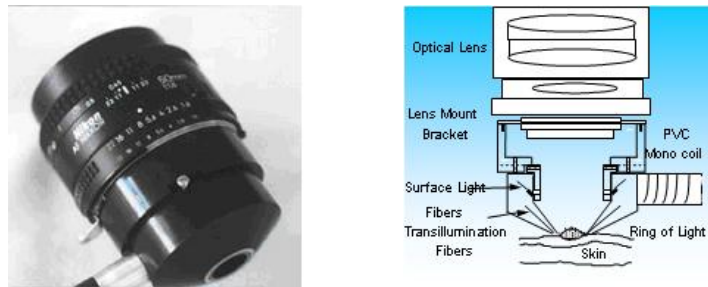
Skin cancer has been the most common and represents 50% of all new cancers detected each year. If detected at an early stage, simple and economic treatment can cure it mostly. Accurate skin lesion segmentation is critical in automated early skin cancer detection and diagnosis systems. In this paper, we propose an Evolution Strategies (ES) based segmentation algorithm to identify the lesion area within an ellipse. The method is applied to 51 XLM and 60 TLM images which have manual segmentation from dermatologists as TRUTH. Unlike most segmentation methods, the proposed ES-based segmentation method can detect the lesion automatically without setting parameters and initial values by trial and error. The method is also compared to algorithms developed in [13,31]. The ES-based method gives comparable accuracy for easily segmented images and much better results for images with either higher noise level, less prominent edge information, or very small size lesions.

*Key words:* melanoma, segmentation, border detection, skin lesion, Evolution Strategies

---

## 1 Introduction

Early detection of cancerous skin lesion has been agreed to be very important due to the wide spread of skin cancer as well as the economic and successful treatment if detected early. For instance, malignant melanomas, the deadliest form of all skin cancers, has cure rate of higher than 95% when detected at an early stage [1]. Segmentation is essential in automatic skin cancer detection and diagnosis systems. Zouridakis, et al. [13,31] developed an automatic system to determine the malignancy based on the size difference in skin lesion images from two imaging modalities: Cross-polarization Epiluminescence Microscopy (XLM) and Transillumination Epiluminescence Microscopy (TLM). Fig.(1) shows the Nevoscope device that can capture both XLM and TLM images and its cross-sectional view. Fig. (2) and Fig. (3) show two pairs image of XLM and TLM from a malignant and a benign skin lesion respectively.



(a) Nevoscope Device      (b) Nevoscope schematic diagram

Fig. 1. Multiple Image Acquisition Modalities by Nevoscope

\* Xiaojing Yuan

*Email addresses:* [xyuan@uh.edu](mailto:xyuan@uh.edu) (Xiaojing Yuan), [zouridakis@uh.edu](mailto:zouridakis@uh.edu) (George Zouridakis), [ning@gmail.com](mailto:ning@gmail.com) (Ning Situ).

*URL:* [www.tech.uh.edu/isgrin](http://www.tech.uh.edu/isgrin) (Xiaojing Yuan).

<sup>1</sup> The project is partially supported by grants from UH-GEAR, NSF, Translite, Inc., and Texas Instrument.

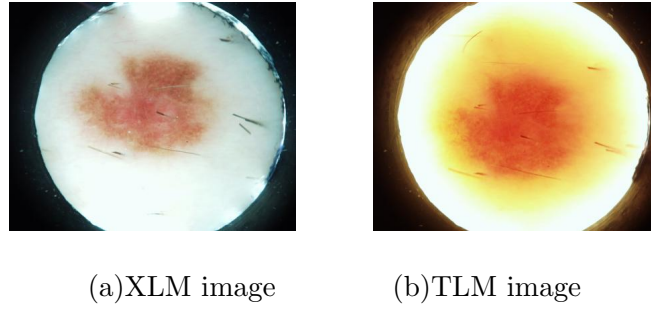


Fig. 2. XLM and TLM images from a malignant skin lesion.

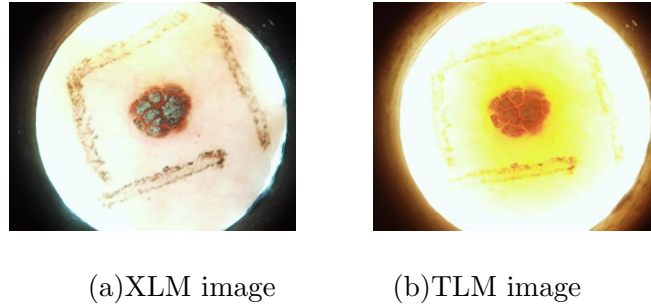


Fig. 3. XLM and TLM images from a benign skin lesion.

The four segmentation methods used to differentiate the lesion area from the background are sigmoid-based thresholding, principle component transform (PCT), PCT based sigmoid thresholding, and fuzzy c-mean clustering. A scoring system then selects the best segmentation result. It has a satisfactory performance with pixel-level error rate less than 15% for 80% of images compared to manual segmentation by dermatologists. However, for the remaining 20% lesion images which have high background noise, weak edge information, or really small lesion size, all four segmentation methods cannot segment the lesion successfully, with error rate higher than 40%. In addition, all segmentation methods performance also heavily depend on manually selected parameters and initial values.

In this paper, we presents a skin lesion segmentation methods based on Evolution Strategies (ES). Like other evolution computation algorithms, such as genetic algorithm, ES algorithm finds the optimum configurations by select-

ing the best candidates from the population in each generation and producing the next generation population by combination and mutation operations. We choose ES algorithm because it is designed for real number function optimization, and will not be affected by uncertainties introduced by quantization errors such as the binary coding for genetic algorithms. In addition, we modified ES algorithm so that it can seek global optimum and get out of the local optimum automatically. To apply the ES algorithm to skin lesion image segmentation, we formulated the segmentation problem as a search problem similar to [30] and designed a special objective function.

Because of the inherent properties of ES algorithm, our ES-based segmentation algorithm has three distinct advantages: (1)its performance does not depend on initialization or threshold values (2)its performance is robust with respect to artifacts and noise; (3)it is based on the regional statistical property of the image. Because of these properties, images fed into the ES-based segmentation algorithm do not need to go through the full pre-processing steps mentioned above. In specific, ES-based segmentation method does not need hair removal procedure. In addition, ES-based method does not require manually selected threshold and is robust to the initial values. The method is validated by experiments on the same data set as used in [13,31]. The experiments show ES based algorithm has a better performance even compared with the best segmentation results selected from four segmentation methods.

The rest of this paper is organized as follows. In the next section, we review some research related to skin lesion image segmentation. After briefly review the general structure of ES algorithm, we proceed to present how we formulate the skin lesion image segmentation as a search problem in Section 3. In Section 4, we present our experiments design and results for the ES-based method. Finally, we present some observations and discussions as well as future direc-

tions for automated skin lesion image segmentation and skin cancer detection to conclude the paper in Section 5.

## 2 Relevant works

Automated systems for detecting melanoma use one imaging modality (such as dermoscopy), mathematical models, and computer algorithms to predict if a skin lesion is melanoma [15]. The general steps of such a system include imaging pre-processing, segmentation, feature extraction and calculation, and classification. The main task of segmentation is to differentiate the lesion from the background. Thresholding [2,19,26,18] and region growing are two simple and most widely used algorithms in the literature. For images with strong contrast, these two techniques usually give good results and the implementation is simple. Clustering algorithms are more robust than simple thresholding and region growing techniques. Orientation sensitive Fuzzy c-mean [15], Density Based Spatial Clustering of Application with Noise(DBSCAN) [5], and JSEG [6] are examples of applying clustering algorithms in lesion segmentation. Melli, et al. [21] compared four clustering algorithms for lesion identification: median cut, k-mean, Fuzzy c-mean, and mean shift. Their results showed that mean shift achieve the best performance in sensitivity and specificity. Active contours or snakes have also been applied to skin lesion segmentation, including geodesic active contours [7,8] and gradient vector flow(GVF) [14]. Both algorithms are edge based schemes. They are sensitive to noisy points and initial conditions, and may fail to detect weaker edge. Content based Markov Random Field (MRF) [10] has also been applied to skin lesion segmentation. Zouridakis, et al [13,31] developed an automatic skin lesion malignance detection system based on size difference of two image modalities [23]: XLM and

TLM. The XLM imaging modality captures only surface pigmentation [4]. The TLM imaging modality can visualize both surface pigmentation and the increased blood volume and vasculature activity around a lesion if present [11,12,22]. Based on angiogenesis, more vascular activity can be observed for cancerous lesions, resulting in bigger lesion area captured by the TLM modality than by the XLM modality. The accuracy of the segmentation determines accuracy of lesion size, thus determines the overall performance of the automatic skin cancer detection system. The best segmentation result is selected from four segmentation methods employed by a scoring system: sigmoid thresholding, principal component transforms (PCT), PCT based sigmoid thresholding, and fuzzy c-mean clustering. The scoring system looks at the differences between segmentation results and the edge strength and selects the one that has majority vote and the strongest edge.

However, these four segmentation methods all have their own limitations, especially when dealing with skin lesion images. The *sigmoid thresholding* method requires that the histogram of the red channel follows the Gaussians distribution. It fails when this condition cannot be satisfied. The *principle component transformation* (PCT) method compares the variance between the lesion and its background in the LAB color space. However, it does not consider any regional statistical property, and in some cases it can not generate enough contrast between the lesion and the background. The *PCT based sigmoid thresholding* method suffers from the same problem as PCT. Moreover, the threshold determined by this method is easily influenced by artifacts. The performance of *fuzzy c-mean clustering based* method is very poor on images with very small lesions. Even though a scoring system based on majority vote mechanism is designed to overcome the limitations of different segmentation methods, for 20% of all lesion images we used, the error rate is still over 40%.

Evolution Strategies (ES) is an evolutionary computation algorithm that designed for real number function optimization and has been applied successfully to different application areas [24,29,30]. Genetic Algorithm(GA), another evolutionary computation technique, is the most popular and has already been applied to image segmentation [3,27] in general and medical image segmentation [16,20] in specific. The major difference is that ES gene evolves in the real number domain, which avoids information loss due to the binary coding representation of GA. Yuan et al. [30] applied ES successfully to multiple feature identification in natural and artificial images. It has also been applied to image registration [29].

To apply the ES algorithm to skin lesion image segmentation, we formulated the segmentation problem as a search problem similar to [30]. The lesion area is segmented by an ellipsoid, whose parameters are optimized by ES algorithm with respect to the defined objective function. The main reason we chose to use an elliptic template for segmentation is because it can be fully defined by five parameters. This makes it easy to implement an ellipsoid region based objective function.

### 3 Materials and Methods

#### 3.1 *Input dataset*

We use the same dataset used in [31]. It consists of 68 pairs XLM and TLM images captured by the same Nevoscope device[4,12] under lighting conditions. An Olympus C2500 (Olympus, Japan) digital camera was attached to the Nevoscope to capture the digitized images, which had a spatial resolution of  $1712 \times 1368$  pixels. In addition, the nevoscope used an optical lens (Nikon,

Japan) to achieve a standard 5X magnification. We validated our ES-based segmentation algorithm on 51 XLM images 60 TLM images using manual segmentation by dermatologist as TRUTH. The remaining lesion images do not show pigmentation and could not even be segmented by a dermatologist[13].

### *3.2 Preprocessing*

Each image undergoes the same preprocessing procedures as detailed in [13,31] including masking, color space conversion, and resizing. As shown in Fig. (2) and Fig. (3), the raw XLM and TLM images acquired by Nevoscope usually have a clear mark made by the doctors to identify the area they would like the image to be taken. In addition, there is a bright ring around the lesion due to the physical mechanism of Nevoscope. To eliminate the ring artifact, a circular ring is determined using the Hough transform [25] and the background external to the ring is masked. Then RGB image is transformed to a grayscale image. We do not perform preprocessing steps such as background correction and hair removal since the ES-based segmentation method is robust to such artifacts. The final step of the preprocessing is resizing the image to convert the rectangular image to square image and to reduce computational cost. We use the bicubic interpolation to maintain the aspect ratio. A lowpass filter of size 11 x 11 is also applied to prevent spatial aliasing. The output of the preprocessing steps are gray scale lesion images of size 256 x 256.

### *3.3 Evolution Strategies*

Evolution Strategies (ES) is a random search based optimization technique. Various applications have shown that when problem are formulated properly,

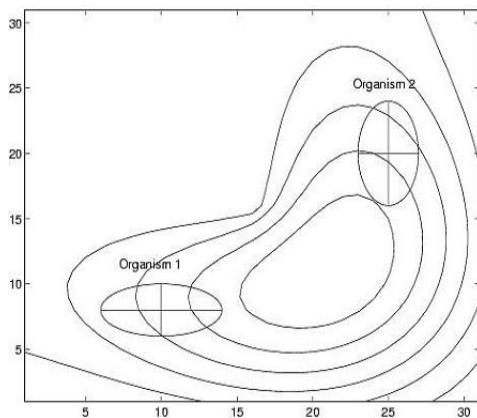
ES can give good results with reasonable time complexity. We chose ES as our optimization methods because of its two properties. First, ES algorithm converge to global optimum instead of local optimum. Second, ES is formulated for optimization of real number functions. The basic elements for using ES include:

- (1) A population (more than one) of candidate solutions (i.e., organisms);
- (2) A measure based on which each member of the population (or candidate solution) will be evaluated, denoted as *objective/fitness* function;
- (3) A “SELECTION” operator that selects the best candidate solutions from population pool based on their fitness value;
- (4) A “MUTATION” operator that makes random changes to a member of the population (corresponding to asexual reproduction in biology evolution);
- (5) A “RECOMBINATION” operator that generates a new organism (or individual solution) by combining “genetic material” from random selected members of the population.

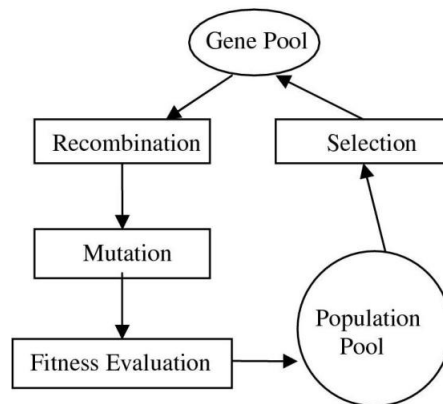
Each organism can be represented by their object variables (which defines the dimension of the organism), and control variables (which defines the standard deviation and auto-correlation of the object variables). Fig.4(a) illustrates two organisms and their vector representations over a hill-climbing problem. The organism 1 and 2 shows the current position in the search space for two organisms in the current generation and their possible directions and step sizes for next generation. Each *object* variable will evolve from generation to generation using mutation and recombination operations. For example, the length of the major axis of the ellipsoid segmentation structure as detailed in section 3.5 is one such object variable. The *control* variables are randomly generated based on Gaussian distribution and the default step size. They determine the randomness of the object variables in the next generation. At the beginning, the

default step size is 1. It decreases during the evolution if the improvement of the fitness values between generations becomes very small while the organisms approach the optimum.

If the optimization problem is defined on two object variables, corresponding to a 2D search space, two examples of the organisms  $\langle 10.0, 8.0; 4.0, 2.0; 0.0 \rangle$  and  $\langle 25.0, 20.0; 2.0, 4.0; 90.0 \rangle$  in the search space are illustrated in Fig.4(a) - the former in the lower left and the latter in the upper right. The axes intersect at the mean and the height/width represent two standard deviations in the appropriate directions. Both organisms are evolving towards the optimum value around  $\langle 20.0, 10.0 \rangle$ . Note that there could be other organisms within the current generation which are not shown here.



(a)ES Organisms illustration



(b)Flowchart of ES

Fig. 4. ES Overview

Fig.4(b) shows the evolution of candidate solutions (i.e., organisms) in one generation of ES. The parent gene pool stores the candidate solutions ( $\mu$ ) selected from population pool. These genes are used as parents to generate candidate solutions or organisms of the next generation. A total of  $\lambda$  organisms (candidate solutions) are generated by undergoing recombination and mutation operations. They are added to the population pool, resulting in  $\mu + \lambda$

organisms for the next generation. The fitness of a newly generated offspring is evaluated using the user defined objective function. Only organisms with good fitness values will be used as parents for the next generation. When using  $(\mu + \lambda)$  selection scheme,  $\mu$  organisms will be selected from all population pool based on their fitness value to be the parent of the next generation. When using  $(\mu, \lambda)$  selection scheme,  $\mu$  organisms will be selected from the  $\lambda$  offsprings as the parent. This finishes the evolution of one generation, as summarized in Fig.4(b). From one generation to the next, the candidate solutions (organisms) evolve to give better and better fitness values. The evolution stops when the fitness values does not improve much (the difference between the fitness value less than an arbitrarily small value  $\varepsilon$  defined by the user:  $\varepsilon \doteq 10^{-6}$ ) from two consecutive generations for 5 times. Another termination criteria based on user defined generation number is used when such convergence condition is difficult to reach. The choice of  $\mu$  and  $\lambda$  will also affect the performance and computational complexity of the evolutionary strategy [24,16].

### *3.4 Principles of automatic skin lesion segmentation by evolutionary computation*

The generic framework of ES-based automatic skin lesion segmentation is shown in Fig.5. The objective is to use ES to divide the whole image into two uniform areas with minimum variation in both regions that conform to the consistency verification rules. The uniformity can be the homogeneity measure of pixel intensity, reflective illuminance, or texture.

Evolutionary computation algorithms, such as Evolution Strategies and Genetic Algorithm, are direct, probabilistic search and optimization procedures rooted in organic evolution. The efficiency (or computational cost) and ro-

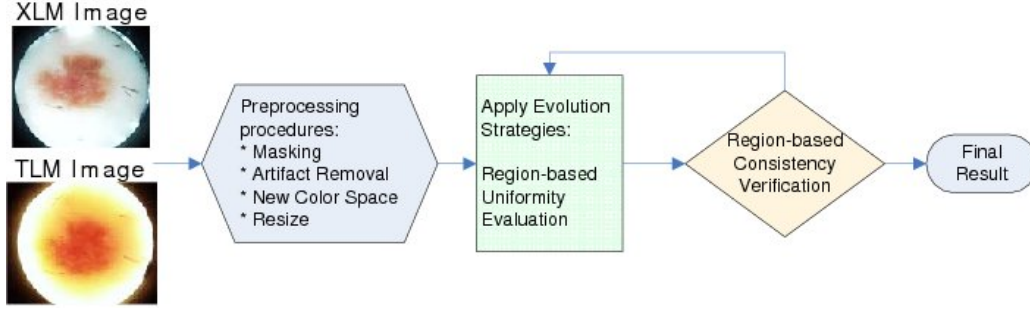


Fig. 5. Framework for the segmentation procedure

bustness(or reliability under varying conditions) of Evolution Strategies to deal with real number numeric optimization problems have been proved in many experiments [24]. We formulated the skin lesion segmentation problem as searching in the image  $I(x,y)$  for the optimum boundary that separates the image into two homogeneous areas (i.e., largest area with lowest variation). Then the consistency verification is applied if user has a priori knowledge about the characteristic of the interesting features in the image. Only qualified results will survive the selection. When the searching process terminated either by fullfilling some convergence criteria or timeout, the best candidate among these qualified solution will be the output optimum.

As shown in Fig.5, after preprocessing, the lesion images are fed into the ES to evaluate the region-based uniformity. Then region-based consistency verification rules are applied until the lesion is segmented.

### 3.5 Skin lesion segmentation problem representation in Evolution Strategies

At the heart of this approach (and a chief contribution of this paper) is transforming the image segmentation problem to a numerical optimization problem and using ellipsoid as the search structure to represent the solution of the optimization problem. The object variables of an ES individual are used to

represent an ellipse corresponding to a candidate boundary that encircles the largest homogeneous region. The uniformity (as measured by to-be-described metrics) of the region both within and outside the ellipsoid structure is the objective value for each candidate.

The ellipsoid search structure is defined by its center, major and minor axis and orientation,  $(X, Y, a, b, \theta)$ . Each organism(candidate solution) in ES can be represented as  $(X, Y, a, b, \theta; \delta_1, \delta_2, \dots, \delta_5; \gamma_1, \gamma_2, \dots, \gamma_{10})$ , where the object variables are defined as the ellipsoid search structure:

$(X, Y)$ : the center of an ellipse;

$(a, b)$ : the minor and major axis radii of an ellipse;

$\theta$ : the rotation angle of an ellipse.

The control variables,  $\vec{\delta}$  and  $\vec{\gamma}$ , have the standard interpretation of defining the hyper-ellipsoid that proscribes the mutation operator.

Although it looks like the ellipse search structure, the 2-dimensional ES representation as shown in Fig.4(a) has a different meaning. The 2-dimensional ES representation shows the current position in the search space, the possible direction and step size for next move. On the other hand, the ellipse search structure is defined on 5-dimensions and therefore it involves a hyper-sphere representation in search space and is difficult to visualize. Furthermore, for image segmentation, besides ellipsoid, different shapes of polygon such as rectangle can be used as search structure.

### 3.6 Objective function

The objective function returns the fitness of an ES organism. We use a region-based objective function as defined in Equation (1) according to the

skin lesion property: the lesion and the background skin have different region statistics. It favors an ellipse that divides the image into two homogenous areas with minimum variation in both regions.

$$F(X, Y, a, b, \theta) = \int_{\omega} |I(x, y) - c_1|^2 dx dy + \int_{\Omega \setminus \omega} |I(x, y) - c_2|^2 dx dy \quad (1)$$

where  $I(x, y)$  is the intensity value of the coordinate  $(x, y)$ ;  $\omega$  is the area enclosed by the ellipse defined by  $(X, Y, a, b, \theta)$ ;  $\Omega$  is the area of the pixels whose intensity value is not zero;  $c_1$  and  $c_2$  represent the average intensity value of the pixels inside and outside  $\omega$  respectively. The area enclosed by the ellipse is calculated as the number of pixels falling inside the ellipse.

To recap, the object variables of an ES organism define the search structure - an ellipse in the search space. In our system, the homogeneity is defined as the difference between the pixel intensity and the average intensity value within the region. The objective function emphasizes the minimum variance at both the region enclosed within the ellipse as well as the region outside the ellipse.

### 3.7 Region based consistency verification

Besides the internal consistency check that determines the termination condition of the ES optimization process and ensure the intensity variance of both regions within and outside the identified ellipse is minimum according to the objective function, we designed region based consistency verification rules based on a priori knowledge about the skin lesion characteristics.

The consistency verification rule is based on the fact that the lesion area always has lower intensity and the goal is to segment the lesion with minimum background enclosed. We examine the smoothed histogram of the segmented

area after applying the ES algorithm. If the first peak (represents the lesion area) is lower than the maximum peak, it means the lesion area is not the dominant feature inside the ellipse. In this case, we apply ES algorithm again. Otherwise, the first peak is the maximum peak, i.e., the lesion is the dominant feature inside the segmented region, and we output it as the final segmentation result.

Based on our experiments, for most XLM images, ES needs to be applied once. That is, the segmented result can pass the consistency check the first time. For most TLM images, ES needs to be applied twice. For the few images whose lesions are very small, ES needs to be applied one more time.

### 3.8 Computational complexity analysis

We analyze the computational complexity for the ES-based segmentation procedures as shown in Fig. 5. The computational time complexity of the pre-processing steps and the consistency verification step is  $O(N^2)$ , where  $N^2$  is the image size.

Theoretical analysis of the computational time complexity of different evolutionary algorithms, including evolution strategies, is still ongoing research [28]. The time consumed for ES varied depends on how many generations it takes to converge. If it takes  $M$  generations to converge, and  $\mu + \lambda$  organism for each generation, the computational complexity is  $O(M \times (\mu + \lambda))$ . As long as  $M$  is much less than  $N^2$ , the ES-based method is more efficient than pixel-based or region-based methods.

We used Pentium(R) 4 CPU 2.26GHz, 1.50 GB of RAM to run the algorithm. The execution time for XLM and TLM images to go through the ES-based segmentation procedures as shown in Fig. 5 is about 15 minutes for those im-

ages that pass the consistency verification the first time. The execution time for those images that need to go through ES algorithm two or more times is about 20 minutes. The pre-processing steps and the randomness of the initial value generated for the first time run of the ES contributes to overhead of the computational time. The computational complexity of the four algorithms in [13,31] is  $O(N^2)$ . Running on the same computer setup, their run time are all within 30 seconds (CPU time).

## 4 Experiments and Results

### 4.1 Experiments Setup

For our experiment, we adapted CMAES [9,17] to perform ES optimization. Our experiment results show that ES guarantees similar performance for different initial values for object and control variables. This demonstrates the robustness of ES algorithm with respect to the initialization. To further improve computational efficiency, we specify the constraints in CMAES to reduce the search area:  $\{(X, Y, a, b, \theta) | (X, Y) \subseteq \{1/9 \times N, 8/9 \times N\}, (a, b) \subseteq \{5, 120\}\}$ , where  $N$  is the size of the image. These constraints are designed based on the following properties of skin lesion images: (1) the lesion area should not exceed the scope of the image; and (2) the lesion area should occupy significant amount of areas near the center of the image. The initial values for object variable of ES organism are generated randomly within the specified search area according to uniform distribution.

We tested  $(\mu + \lambda)$  selection and  $(\mu, \lambda)$  selection with same population size setting - 5 for the parent population and 30 for the descendant population - on 10 images. For the skin lesion segmentation problem, similar performance

and the computational time are achieved by both selection scheme. We decided to use  $(\mu, \lambda)$  for all the images. The recombination operators on object variables and control variables are discrete recombination on object variables and panmictic intermediate recombination of control variables, respectively. A convergence criterion is tested after each 10 generations and a maximal computation time of 10 seconds (CPU time) is set to terminate the search in case the convergence criterion is not met.

To quantitatively evaluate the performance of the ES-based segmentation method and compare the results with the previous works, we adopted the error ratio used in [13,31]. An error rate  $E$  is defined as the normalized agreement of segmentation results and the reference. Let  $c$  denote the border of the segmentation result and  $c_r$  is the reference border. Notation  $\mathcal{A}(c)$  gives the set of pixels enclosed by border  $c$ .  $\mathcal{A}(c) \oplus \mathcal{A}(c_r)$  defines the set of pixels belong to  $\mathcal{A}(c)$  or  $\mathcal{A}(c_r)$  but not in both (which means the exclusive or operation of two sets). The error rate is formulated as follows:

$$E = \frac{|\mathcal{A}(c) \oplus \mathcal{A}(c_r)|}{|\mathcal{A}(c)| + |\mathcal{A}(c_r)|} \quad (2)$$

where  $|A|$  denotes the cardinality of the set  $A$ .

The error rate will be 1 if  $\mathcal{A}(c)$  and  $\mathcal{A}(c_r)$  enclose totally different areas. It will be 0 if  $\mathcal{A}(c)$  and  $\mathcal{A}(c_r)$  enclose the same areas. The proposed ES-based algorithm will be compared with the algorithms developed in [13,31] using the same data set.

## 4.2 Experiments Results

The ES-based segmentation method is applied to 51 XLM images and 60 TLM images which have manually segmentation by certified dermatologist. These manual segmentation are treated as true values, and we validate our ES based segmentation algorithm by comparing its results with the manually segmented results as well as four segmentation methods previously developed in [13,31]: I. Sigmoid; II. PCT; III. PCT plus Sigmoid; and IV. Fuzzy c-mean. Compared with these methods, the experiment results show that ES-based method performs better and is more robust when applying to images with higher noise level, very small lesion, or weak edge, which we defined as “difficult” images.

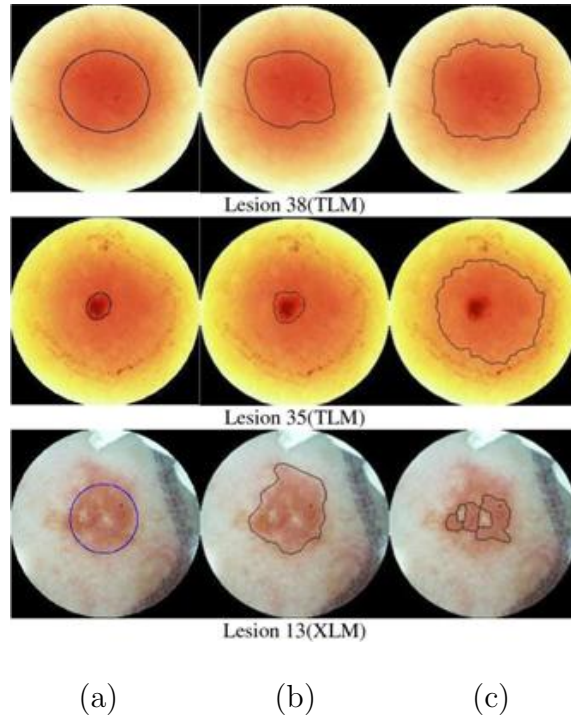


Fig. 6. Comparing ES (column (a)), dermatologist (column (b)) , and [13]’s results (column (c)).

Results shown in Fig.6 demonstrate much better segmentation results from

ES-based algorithm for Lesion 38(TLM), 35(TLM), and 13(XLM). In Fig.6, each row shows the segmentation results of one “difficult” XLM or TLM image: the first column shows the ES-based method results; the middle column shows manual segmentation by a certified dermatologist; and the last column shows the best segmentation results selected based on the scoring system developed in [13,31]. The edge of the lesion 38 is very vague; the lesion 30 is very small; and lesion 13 is lesion clusters with holes in between. With combination of the objective function in Eq.(1) and the consistency verification criteria, ES-based method is not affected by the edge strength (lesion 38), size of the lesion(lesion 35), and holes in the middle of the lesion (lesion 13), as compared with other segmentation methods. Table 1 shows the error rate comparison of these “difficult” images between the ES-based method and the best segmentation result from the four segmentation methods selected by the scoring system developed in [13,31]. From Table 1, we can see the error reduction from the ES-based method and the best result of the “difficult” images ranges from 45.77% to 84.71%, which is significant improvement.

Algorithm	ES	Scoring System	Error Reduction %
TLM #38	12.12%	22.35%	45.77%
TLM #72	6.48%	42.38%	84.71%
XLM #13	17.6%	45.05%	60.93%
Average	12.07%	36.59%	67.01%

Table 1

Error ratio for images in Fig.6.

Table 2 shows the average error rate comparison the ES-based method

Table 2

Average error ratio for XLM and TLM images of the four algorithms and ES.

Algorithm	I	II	III	IV	ES
XLM	N/A	17.96%	15.58%	13.57%	14.82%
		(10.8%)	(13.0%)	(10.0%)	(7.0%)
TLM	23.09%	N/A	19.22%	16.57%	16.71%
	(22.1%)		(18.0%)	(18.3%)	(12.3%)

and the the four segmentation methods for other XLM and TLM skin lesion images.

As shown in Table 2, for most of the 110 skin lesion images, where the edge is well defined and the artifact and noise level are low, ES-based method achieves compatible result by running ES one time. The standard deviations are much lower than those from the other four segmentation methods because of its robustness to high noise and artifacts. It is worth pointing out that for the four segmentation methods (I - IV), besides the pre-processing steps described in Section 3.2 such as masking, color space conversion, and resizing, other steps such as median filtering, background correction, and hair removal have been used before the four segmentation methods are used [13,31]. In spe-

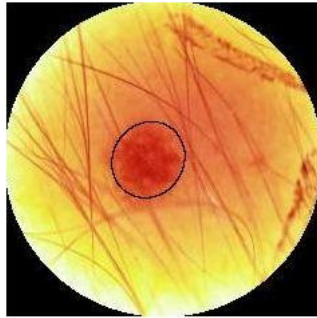


Fig. 7. ES-based algorithm able to segment the lesion area even with a lot of hair.

cific, Fig.7 shows one instance where too much hair prevents any of the four segmentation methods detect the lesion region correctly even after the hair removal preprocessing.

However, the performance of ES is limited by the search structure we selected, i.e., ellipsoid. As shown in Fig.8, though ES-based method correctly identified and segmented the lesion area, the arbitrary shape of the manual segmentation by the dermatologists and the definition of pixel based error ratio (Eq.2) dampened the ES performance number.

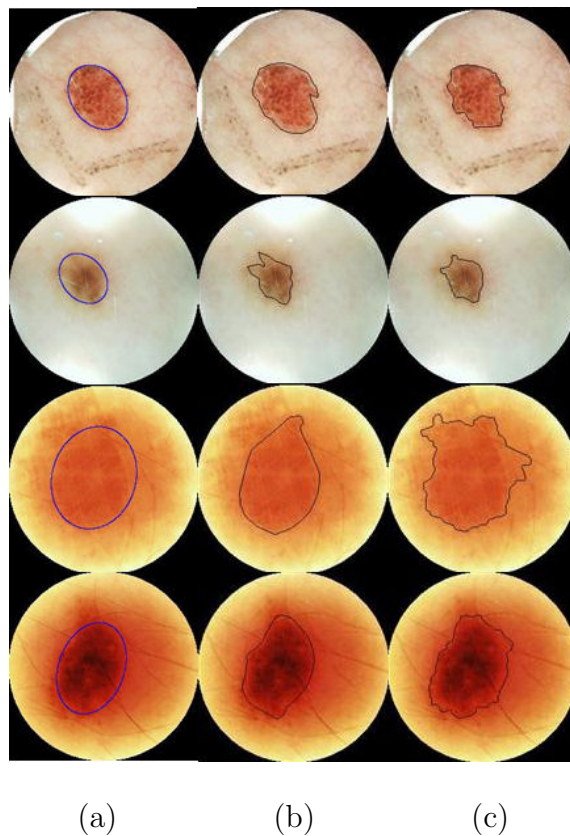


Fig. 8. Comparing ES(col. (a)), dermatologist(col. (b)) , and [13]’s results(col. (c)).

## 5 Conclusion and discussion

In this paper, we present a generic framework for automatic skin lesion segmentation based on Evolution Strategies. We transform the skin lesion seg-

mentation problem into a numerical optimization problem and use ES with an ellipsoid search structure. We designed objective function that favors the enclosure that separates the whole image into two homogeneous regions. Based on the characteristics of skin lesion images, histogram based consistency verification rule is used to automatically refine the segmentation results.

Experiments were done for 60 TLM and 51 XLM images with TRUE value from one certified dermatologist. Results demonstrate that ES-based algorithm is more robust to artifacts and noise. It does not require any user input parameters, such as threshold, and its performance does not depends on initial values. However, due to the ellipsoid search structure, it does not give detailed segmentation results. On the other hand, the proposed ES-based segmentation framework is flexible to adopt other objective functions and search structures. In addition, texture information can be added to improve the computational efficiency.

In the future, we plan to incorporate some edge and texture information to further improve the segmentation results and computational efficiency.

## References

- [1] Anonymous, Cancer facts & figures 2002 (2002).
- [2] G. Betta, G. D. Leo, G. Fabbrocini, A. Paolillo, M. Scalvenzi, Automatic application of the '7-point checklist' diagnosis method for skin lesions: Estimation of chromatic and shape parameters,, in: Proceedings of the IEEE Instrumentation and Measurement Technology Conference (IMTC05), Vol.3, May 2005.
- [3] S. M. Bhandarkar, H. Zhang, Image segmentation using evolutionary computation, IEEE Trans. on Evolutionary Computation 3 (1) (1999) 1–21.

- [4] M. Binder, Skin examination device, US Patent Number 6,032,071, Published in 2000.
- [5] M. E. Celebi, Y. A. Aslandogan, P. R. Bergstresser, Mining biomedical images with density-based clustering, in: International Conference on Information Technology: Coding and Computing, ITCC 2005, Proceedings, IEEE, 2005.
- [6] M. E. Celebi, Y. A. Aslandogan, P. R. Bergstresser, Unsupervised border detection of skin lesion images, in: International Conference on Information Technology: Coding and Computing, ITCC 2005, Proceedings, IEEE, 2005.
- [7] D. H. Chung, G. Sapiro, Segmenting skin lesions with partial-differential-equations-based image processing algorithms,, in: International Conference on Imaging Processing,ICIP 2000, Proceedings, vol. 3, IEEE, 2000.
- [8] D. H. Chung, G. Sapiro, Segmenting skin lesions with partial-differential-equations-based image processing algorithms, IEEE Transactions on Medical Imaging 19 (7) (2000) 763–767.
- [9] CMAE, <http://www.bionik.tu-berlin.de/user/niko/cmaes.m>, accessed in oct. 2006.
- [10] H. Deng, D. A. Clausi, Unsupervised image segmentation using a simple mrf model with a new implementation scheme,, in: International Conference on Pattern Recognition, ICPR 04, Proceedings, USA, Aug. 23-26, vol. 2, IEEE, 2004.
- [11] M. Detmar, Tumor angiogenesis, Journal of Investigative Dermatology Symposium Proceedings 5 (1) (2000) 20–23.
- [12] P. Dhawan, Apparatus and method for skin lesion examination, US Patent Number 5,146,923, Published in 1992.
- [13] M. Doshi, Automated segmentation of skin cancer images, Master’s thesis, University of Houston (May 2004).

- [14] B. Erkol, R. Moss, R. Stanley, W. Stoecker, E. Hvatum, Automatic lesion boundary detection in dermoscopy images using gradient vector flow snakes,, *Skin Research and Technology* 11 (1) (2005) 17–26.
- [15] H. Ganster, A. Pinz, R. Rohrer, E. Wildling, M. Binder, H. Kittler, Automated melanoma recognition, *IEEE Trans. on Medical Imaging* 20 (3) (2001) 233–239.
- [16] P. Ghosh, M. Mitchell, Segmentation of medical images using a genetic algorithm, in: M. Cattolico (ed.), *Genetic and Evolutionary Computation Conference, GECCO 2006, Proceedings, Seattle, Washington, USA, July 8-12, 2006*, ACM, 2006.
- [17] N. Hansen, *The CMA Evolution Strategy: A Tutorial* (Nov. 2005).
- [18] R. Jailani, H. Hashim, M. N. Taib, S. Sulaiman, Border segmentation on digitized psoriasis skin lesion images, in: *2004 IEEE Region 10 Confernece TENCON*, Nov. 2004.
- [19] E. Maglogiannis, C. Caroni, S. Pavlopoilos, V. Karioti, Utilizing artificial intelligence for the characterization of dermatological ages, in: *NNESMED, 2001*.
- [20] C. McIntosh, G. Hamarneh, Genetic algorithm driven statistically deformed models for medical image segmentation, in: M. Cattolico (ed.), *Genetic and Evolutionary Computation Conference, GECCO 2006, Proceedings, Seattle, Washington, USA, July 8-12, 2006*, ACM, 2006.
- [21] R. Melli, C. Grana, R. Cucchiara, Comparison of color clustering algorithms for segmentation of dermatological images,, in: J.M.Reinhardt, J.P.W.Pluim (eds.), *SPIE Medical Imaging:Image Processing*,, vol. 6144, 2006.
- [22] N. Mullani, R. Talpur, N. Apisarnthanarax, M. Weinstock, R. Drugge, C. Ahn, V. Prieto, M. Duvic, Side-transillumination epiluminescence imaging

for diagnosis of dysplastic nevi and melanoma a comparison to oil and cross-polarization epiluminescence imaging, in press.

- [23] Nevoscope, <http://www.nevoscope.com>.
- [24] H. P. Schwefel, *Evolution and Optimum Seeking*, Wiley Interscience and John Wiley & Sons, New York, 1995.
- [25] M. Sonka, V. Hlavac, R. Boyle, *Image processing, analysis, and machine vision*, 2nd ed., Brooks and Cole Publishing, 1998.
- [26] K. Taouil, N. B. Romdhane, Automatic segmentation and classification of skin lesion images,, in: *The 2nd International Conferences on Distributed Frameworks for Multimedia Applications*, May 2006.
- [27] C. Veenman, M. Reinders, E. Backer, A cellular coevolutionary algorithm for image segmentation, *IEEE Transactions on Image Processing* 12 (3) (2003) 304–316.
- [28] X. Yao, J. E. Rowe, J. He, Computational complexity analysis of evolutionary algorithms, <http://gow.epsrc.ac.uk/ViewGrant.aspx?GrantRef=EP/C520696/1>.
- [29] X. Yuan, J. Zhang, B. P. Buckles, Evolution strategies based image registration via feature matching., *Information Fusion* 5 (4) (2004) 269–282.
- [30] X. Yuan, J. Zhang, X. Yuan, B. P. Buckles, Multi-scale feature identification using evolution strategies, *Image and Vision Computing Journal* 23 (6) (2005) 555–563.
- [31] G. Zouridakis, M. Doshi, N. Mullani, Early diagnosis of skin cancer based on segmentation and measurement of vascularization and pigmentation in nevoscope images, in: *Proceedings of the 26th Annual International Conference of the IEEE EMBS*, IEEE, 2004.